

Responses of the phototransduction cascade to dim light

(microcalorimetry/rhodopsin/transducin/rhodopsin kinase/recoverin)

GWENN LANGLOIS*, CHING-KANG CHEN†, KRZYSZTOF PALCZEWSKI‡, JAMES B. HURLEY†, AND T. MINH VUONG*§

*Institut de Pharmacologie Moléculaire et Cellulaire, Centre National de la Recherche Scientifique, 660 route des Lucioles, F06560 Valbonne, France; the

†Department of Biochemistry and Howard Hugues Medical Institute, University of Washington, Seattle, WA 98195; and the ‡Departments of Ophthalmology and Pharmacology, University of Washington, Seattle, WA 98195

Communicated by Denis Baylor, Stanford University School of Medicine, Stanford, CA, January 4, 1996 (received for review September 10, 1996)

ABSTRACT The biochemistry of visual excitation is kinetically explored by measuring the activity of the cGMP phosphodiesterase (PDE) at light levels that activate only a few tens of rhodopsin molecules per rod. At 23 °C and in the presence of ATP, the pulse of PDE activity lasts 4 s (full width at half maximum). Complementing the rod outer segments (ROS) with rhodopsin kinase (RK) and arrestin or its splice variant p44 does not significantly shorten the pulse. But when the ROS are washed, the duration of the signal doubles. Adding either arrestin or p44 back to washed ROS approximately restores the pulse width to its initial value, with p44 being 10 times more efficient than arrestin. This supports the idea that, *in vivo*, capping of phosphorylated R* is mostly done by p44. When myristoylated (14:0) recoverin is added to unwashed ROS, the pulse duration and amplitude increase by about 50% if the free calcium is 500 nM. This effect increases further if the calcium is raised to 1 μM. Whenever R* deactivation is changed—when RK is exogenously enriched or when ATP is omitted from the buffer—there is no impact on the rising slope of the PDE pulse but only on its amplitude and duration. We explain this effect as due to the unequal competition between transducin and RK for R*. The kinetic model issued from this idea fits the data well, and its prediction that enrichment with transducin should lengthen the PDE pulse is successfully validated.

The electrical response of a dark-adapted retinal rod exhibits the two remarkable features of single-photon sensitivity and highly stereotyped kinetics (1), which ultimately must be traced to the underlying amplification cascade. During activation of this cascade, the heterotrimeric G protein, transducin (TβγTα-GDP) upon being activated by photoexcited rhodopsin (R*) via a GDP/GTP exchange, associates with and turns on the cGMP phosphodiesterase (PDE). Hydrolysis of cGMP by active PDE (PDE*) causes closure of the cGMP-gated channels and hyperpolarization of the rod (2). To terminate this electrical signal, breakdown of cGMP must stop, and its resynthesis must be stimulated. Deactivation of the amplification cascade is needed to end cGMP hydrolysis; PDE* is turned off when Tα-GTP hydrolyzes its own GTP (3). R* is deactivated upon being phosphorylated by rhodopsin kinase (RK) and capped by arrestin (4). Thus, the time course of cGMP hydrolysis or, equivalently, PDE activity should reveal much about the amplification cascade at the root of the photoreponse of the rod cell. What is the kinetics of this PDE activity under conditions resembling those of a living rod cell? What does it tell us about the lifetime of R*? Recoverin is thought to modulate the deactivation of R* by interacting with rhodopsin kinase in a calcium-dependent manner (5, 6). How would recoverin affect the kinetics of PDE*? The recently described 44-kDa splice variant of arrestin, p44, is reported to cap phosphorylated R* much more efficiently than does

arrestin (7, 8). How would this difference manifest itself kinetically?

A physiologically relevant measurement of PDE activity must meet two challenges. First, this activity can only be measured from suspensions of highly disrupted rod outer segment (ROS) fragments, where the loss of soluble and peripheral proteins is a major concern. During preparation of ROS, there is loss at several washing steps, especially of the highly soluble arrestin. During the experiment itself, if the ROS concentration is less than 25 μM rhodopsin, peripheral proteins such as transducin and PDE get spontaneously solubilized (9). Second, the pHmetric method is widely used to measure PDE activity (10), but it lacks the required sensitivity. A dark-adapted rod saturates electrically when only a few tens of its 10⁸ rhodopsin molecules are photoactivated. At such light levels, the pH electrode detects nothing. We deal with potential losses of proteins by using a high concentration of membrane to prevent spurious solubilization of peripheral species and by supplementing the ROS with purified or recombinant proteins such as arrestin, p44, RK, and recoverin. As for the issue of sensitivity, the novel technique of time-resolved microcalorimetry (3) is used to follow the time course of PDE* at illumination levels comparable with those seen by a live, dark-adapted rod.

MATERIALS AND METHODS

Bovine rod outer segments are prepared from fresh retinas under dim red light (11), and the pellets stored at -80 °C. The ROS are resuspended in 100 mM KCl, 1 mM MgCl₂, 100 μM GTP, 2 mM NADPH, 1 mM DTT, 50 mM Hepes, pH 7.5, and disrupted by passage through a 26-gauge, 51-mm Hamilton syringe needle. This concentrated stock suspension (250–300 μM rhodopsin) is kept on ice for ~1.5 h to allow any contaminating R* to decay away. When needed, the ROS are washed twice in 100 mM KCl, 1 mM MgCl₂, 1 mM DTT at a membrane concentration of 75 μM rhodopsin; 1 mM EGTA is present in the first wash. This protocol removes most of the arrestin and recoverin while preserving as much as possible peripheral proteins such as transducin and PDE. After washing, the ROS are resuspended, disrupted, and incubated on ice as described above. All operations are carried out under IR illumination. Calcium buffers are prepared according to the method of Tsien and Pozzan (12). HoloTransducin is extracted from bovine ROS and purified on a Superose-12 gel filtration column (Pharmacia Biotech) and concentrated on Centricon-30. Arrestin and its splice variant, p44, are purified from bovine ROS (7, 13). Rhodopsin kinase is expressed in a baculovirus-sf9 system and purified on a recoverin affinity column (14). Myristoylated (14:0) recoverin is expressed in *Escherichia coli* and purified as described (15).

Abbreviations: R, rhodopsin; R*, photoexcited R; PDE, phosphodiesterase; PDE*, active PDE; RK, R kinase.

§To whom reprint requests should be addressed. e-mail: vuong@unice.fr.

The publication costs of this article were defrayed in part by page charge payment. This article must therefore be hereby marked "advertisement" in accordance with 18 U.S.C. §1734 solely to indicate this fact.

The microcalorimeter is slightly improved from an earlier version (3). Briefly, it uses a pyroelectric film of poled polyvinylidene fluoride that dilates upon being heated and generates a displacement current, which is directly proportional to the derivative of the heat produced. This current is on the order of 0.1 pA and is converted to voltage with an AD549LH operational amplifier (Analog Devices, Norwood, MA). Before being digitized at 50 samples per second, the signal is filtered with an RC circuit whose 220-ms time constant determines the overall temporal resolution of the instrument. The volume of the sample chamber is 300 μ l; its surface area is 680 mm². The sample's thickness of only \sim 0.4 mm allows for a homogeneous illumination of the ROS fragments. The actinic light comes from a photographic flash that is filtered with a narrow band [10 nm full width at half-maximum (FWHM)] 500-nm interference filter and attenuated with a series of neutral density filters. To correct for the \pm 10% variation in flash intensity, a small fraction of the light pulse is collected with a photodiode and used to normalize the data. The microcalorimeter is calibrated by heating a sample of Red Ponceau dye ($A_{500} = 1$) with a flash whose intensity is measured with a calibrated photodiode (13DSI009, Melles-Griot, Irvine CA). Since the photodiode's active area of 31 mm² is smaller than the area of the chamber, the latter is sampled at nine evenly distributed spots. The calibration factor is 1 mV = 0.17 μ cal/s. The impulse response of the instrument is also obtained during this calibration.

Nucleotides and exogenous proteins such as arrestin, p44, or RK are added to the adequate volume of ROS stock in total darkness. The final buffer contains 100 mM KCl, 1 mM free Mg²⁺, 1 mM DTT, 50 mM Hepes, pH 7.5, 1 mM GTP·Mg²⁺, 10 mM cGMP, 3 mM ATP·Mg²⁺ (unless otherwise noted), and the needed Ca²⁺ buffer. ROS concentrations are always much greater than 25 μ M rhodopsin. The sample is gently injected into the microcalorimeter. The time between addition of nucleotides to the ROS and the first flash is 10 min. The temperature of the sample chamber is 22.5 °C. All experiments are repeated at least twice, with similar results.

RESULTS AND DISCUSSION

Complementation of Unwashed ROS with Arrestin, RK, and p44. A typical heat pulse elicited from a ROS sample containing GTP, cGMP, and ATP is shown in Fig. 1A (trace 1). The signal disappears when either cGMP or GTP is omitted and is drastically reduced by the PDE inhibitor Zaprinast (not shown). The observed heat indeed comes from cGMP hydrolysis by transducin-activated PDE. The amplitude of the signal increases linearly with the flash intensity, while its shape is unchanged. At the low light levels used here (5–70 R*/rod), the fractions of PDE and transducin that get activated must be tiny. One expects each PDE* to harbor just one T α -GTP and to have a turnover number of 500. This is half of the maximum value of 1000 (16), which arises when each PDE* binds to two T α -GTPs. We compute the PDE* scale of Fig. 1 using the turnover number of 500 and the -11.2 Kcal/mol enthalpy of cGMP hydrolysis (17). On this scale, the peak amplitude of the control trace in Fig. 1A is only 1.4 nM PDE*, a mere 0.1% of the total PDE pool. This experiment establishes the feasibility of probing in real time the biochemistry of the amplification cascade at physiological light levels.

But does the biochemistry of these ROS fragments reflect the situation *in vivo*, given the potential loss of proteins that help deactivate the cascade? The loss of soluble arrestin is substantial. When ROS are washed as described above, the first supernatant contains arrestin, among many other proteins (Fig. 1 gel). Densitometry of this band of arrestin reveals that its concentration in the control aliquot of Fig. 1A is \sim 3 μ M. In an intact, dark-adapted outer segment, the arrestin level is thought to be 10–15 μ M. We thus add 8 μ M arrestin, which

does nothing to the kinetics of the signal; traces 1 and 2 in Fig. 1A are superimposable. Increasing this exogenous arrestin to as much as 20 μ M has little or no effects (data not shown). As for RK and p44, it is not clear how much loss there is during the preparation of the ROS. The amounts of RK and p44 in intact rods are estimated to be 1–2% of rhodopsin (K.P., unpublished data). Rhodopsin kinase is farnesylated and should be well preserved, like transducin and PDE. Given the electrostatic interaction between the disc membrane and p44 (7), its loss could be higher. Conservatively, we assume that half of the original RK and most of the p44 were gone during preparation of the ROS. In Fig. 1A, the addition of 520 nM (0.43% R) of RK and 8 μ M arrestin (trace 4) only causes a slight decrease in the peak amplitude as compared with the control. As for the rising and falling slopes, they are unchanged. This invariance reflects the underlying chemistry and not a limitation in the instrument's time response since flashes 5–10 times brighter than those used here elicited proportionately steeper rising phases (data not shown). It looks like the smaller peak amplitude is not due to a steeper falling slope or a lessened rising slope but to an earlier onset of deactivation processes, which prematurely terminate the activation phase. The effect is slight as the FWHM of the pulse changes from 4.8 to 3.6 s.

In Fig. 1B, the addition of 1 μ M p44 (1% R) produces somewhat more of an effect than the 8 μ M arrestin: a slight decrease in the rising slope and in the peak amplitude (trace 2 versus trace 1). This rising slope is further reduced if the p44 level is made comparable with that of transducin (data not shown). This influence of p44 on the rising slope is consistent with the recent finding that p44 also binds to nonphosphorylated R* (7). If such binding was tight enough, the amount of R* available for transducin activation would be smaller, which is equivalent to having less light and therefore a shallower rising slope. The further addition of 520 nM (0.43% R) of RK produces the same effect as above: strict preservation of the rising and falling slopes but a smaller peak amplitude because deactivation now occurs earlier. As in Fig. 1A, the effect is small; the FWHM changes from 5.5 s in the control to 3.8 s with the addition of RK and p44. In these experiments, the requirement for ATP is crucial. Its absence causes PDE* to linger much longer (trace 4), which we attribute to a less efficient deactivation of R* when GTP is used by RK in lieu of ATP. The rising slope is again preserved whether R* quenching is encouraged by the inclusion of ATP or discouraged by its omission.

Partial Reconstitution of Washed ROS with RK and Arrestin. In Fig. 1C, the ROS are washed to remove most of the endogenous arrestin and recoverin. A careful examination of the gel reveals also some loss in p44 and RK. Deactivation is now much less efficient, and the PDE* pulse is lengthened by more than 2-fold as compared with the signal with unwashed ROS. When 1 μ M arrestin is added to these washed ROS, the falling slope becomes steeper and the PDE* pulse shortens a little. The addition of 120 nM (0.25% R) RK causes a significant decrease in amplitude but no changes in the rising slope and pulse width. As a result, the downward slope of the signal with RK is significantly shallower than in the control. R* deactivation in these washed ROS would not be limited by phosphorylation but rather by a lack of arrestin. Indeed, when both arrestin and RK are added (trace 4), the falling slope becomes steeper, resulting in a significant shortening of the pulse; the 7-s FWHM of trace 4 approaches the value obtained with unwashed ROS. In Fig. 1D, washed ROS were complemented with a smaller level of RK (60 nM or 0.13% R) and increasing amounts of arrestin, resulting in increasingly shorter pulses and further indicating that the deactivation of R* is limited here at the capping step. The FWHM of the sample with the highest level of added arrestin is 6 s. Hence, with a small amount of RK and a sufficiently high level of arrestin, we

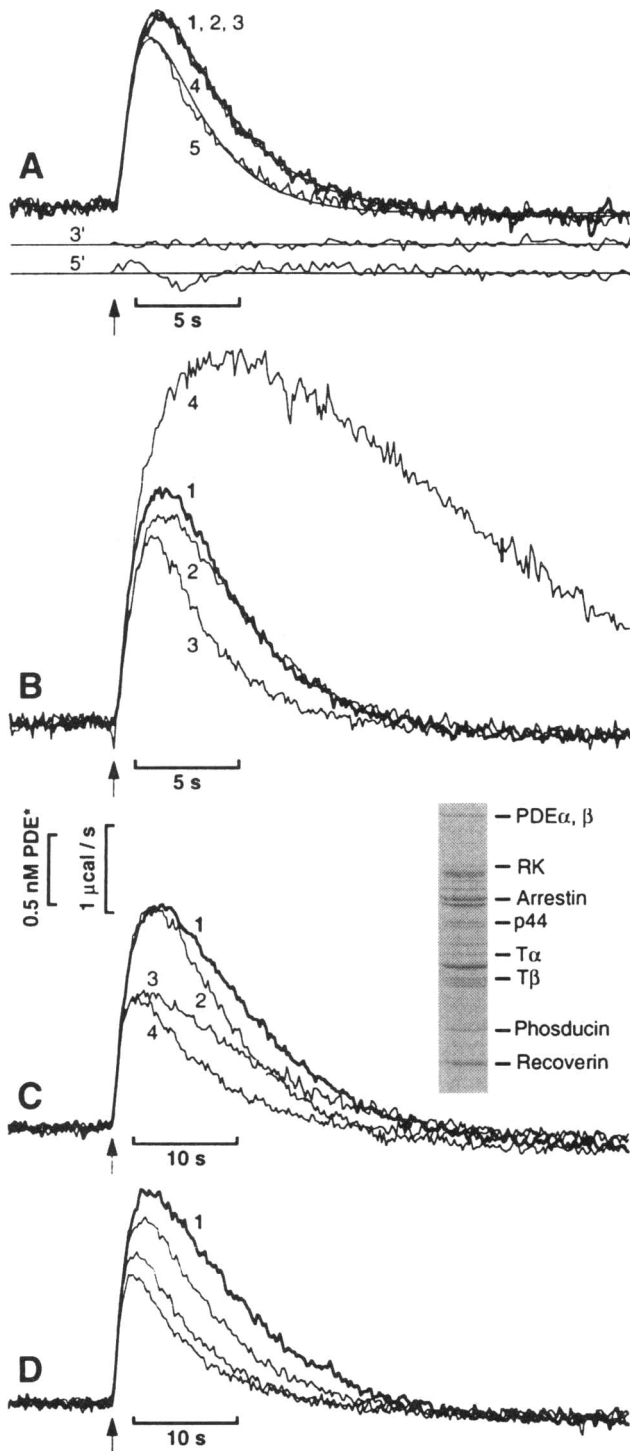


FIG. 1. Complementation and partial reconstitution with arrestin, p44, and RK. All samples contained 10 nM free Ca^{2+} . The thick traces (labeled 1) are controls with no proteins added. Arrows provide the flash timing. (A) The ROS (113 μM rhodopsin) were unwashed. $[\text{R}^*] = 45 \text{ R}^*/\text{rod}$. The test aliquots contained 8 μM exogenous arrestin (trace 2) or 8 μM arrestin + 520 nM RK (trace 4). Traces 3 and 5 are fits to traces 1 and 4, respectively (see text); their residuals are traces 3' and 5'. (B) The ROS concentration and light level are identical to those in A. ATP was omitted from the aliquot of trace 4. The aliquots contained no added proteins (traces 1 and 4), 1 μM p44 (trace 2), or 1 μM p44 + 520 nM RK (trace 3). (C) The ROS (49 μM rhodopsin) were washed twice (see text). $[\text{R}^*] = 66 \text{ R}^*/\text{rod}$. The test aliquots contained 1 μM arrestin (trace 2), 120 nM RK (trace 3), or 120 nM RK + 1 μM arrestin (trace 4). The supernatant from the first wash was run on a 12% SDS gel. The amounts of endogenous arrestin and recoverin were obtained by densitometry of this gel (see text). (D)

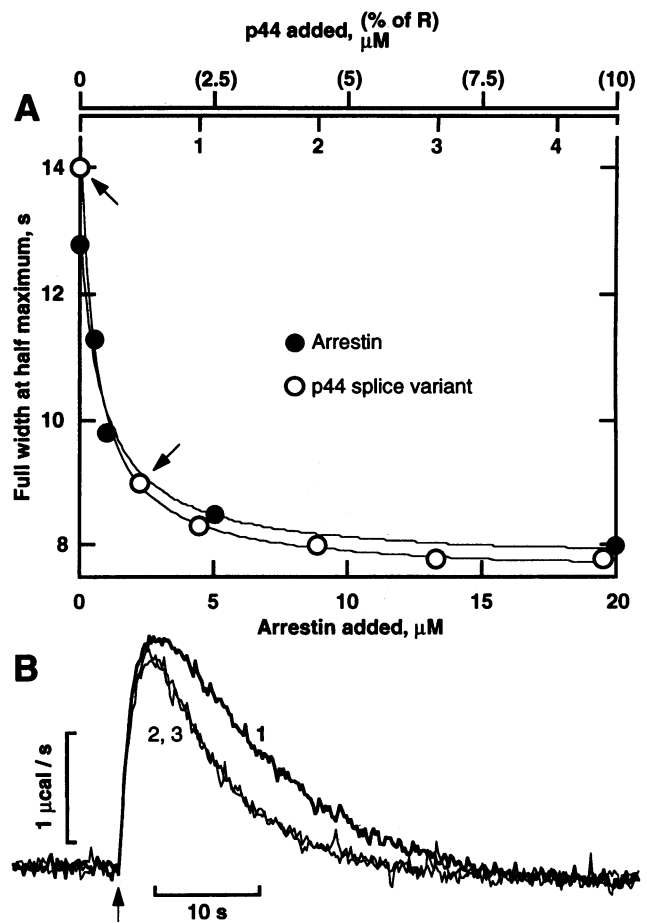


FIG. 2. Comparing arrestin to p44. $[\text{free Ca}^{2+}] = 10 \text{ nM}$; $[\text{R}^*] = 66 \text{ R}^*/\text{rod}$. (A) Washed ROS (45 μM rhodopsin) were complemented with increasing amounts of arrestin (closed circles) or p44 (open circles). $[\text{R}^*] = 66 \text{ R}^*/\text{rod}$. The full width at half-maximum of each PDE* pulse is plotted as a function of added proteins. Note the difference in scale for arrestin and p44. Signals from the aliquots containing 0 and 0.5 μM exogenous p44 (arrows) are shown in B. (B) Traces 1 and 2 are from the two aliquots of the p44 dose-response curve of A that contained 0 and 0.5 μM p44, respectively. A third aliquot (trace 3) contained 5 μM arrestin.

can essentially reverse the reduction in R^* deactivation incurred by washing the ROS. From these data, we reach three conclusions. (i) The deactivation kinetics observed with unwashed ROS is already maximal as enrichment with RK and arrestin or p44 does not drastically reduce the PDE* pulse width. (ii) The RK and arrestin used in such enrichment are indeed active as judged by their effects on washed ROS. (iii) To the extent that in these washed ROS the deactivation of R^* is limited at the capping step, we now have a means to ascertain if p44 is indeed more efficient than arrestin in this function.

Comparing Arrestin with Its Splice Variant, p44. In the experiments of Fig. 2, increasing amounts of p44 or arrestin are added to aliquots of washed ROS. The FWHM of the resulting PDE* pulse is plotted as a function of added p44 or arrestin (Fig. 2A). In both sets of experiments, the ROS concentration is identical (45 μM rhodopsin), yet the arrestin dose-response curve saturates at 5–10 μM , while the p44 curve does so at only 1–2 μM (2–4% R). This significant difference in efficiency is also seen in Fig. 2B where 0.5 μM p44 shortens the PDE* pulse to exactly the same extent as 5 μM arrestin. With phosphor-

[Washed ROS] = 41 μM rhodopsin; $[\text{R}^*] = 66 \text{ R}^*/\text{rod}$. The test aliquots contained 60 nM RK plus, from top to bottom, 1, 5, and 20 μM arrestin.

ylated R* and p44 being both membrane proteins, their affinity for each other is a straightforward concept. On the other hand, a notion of affinity between the soluble arrestin and the membrane-bound phosphorylated R* is much harder to define. Consequently, one cannot say here that the affinity of p44 for phosphorylated R* is 10 times that of arrestin. However, the more general conclusion that p44 is much more efficient than arrestin in capping phosphorylated R* is very much valid. Perhaps the simplest reason for this 10-fold difference in efficiency is the higher effective concentration of p44 on account of its being membrane-localized (18). This large difference in efficiency permits an interesting interpretation for the observation of Fig. 1, where the addition of 8 μM arrestin to unwashed ROS has no effects even though the original arrestin level is only 3 μM . The capping of phosphorylated R* in these samples would be mostly due to the action of p44, which is abundant enough to saturate the effect so that further enrichment with either arrestin or p44 does not speed up the PDE* pulse. This comparison between arrestin and p44 strongly suggests that at low light levels, in a live rod, capping of phosphorylated R* is mostly performed by the splice variant. The more abundant arrestin would help quench the large amount of R* produced in bright light.

Delay of Quenching by High Calcium and Myristoylated Recoverin. We now turn to the effects of calcium and of the calcium-binding protein recoverin on the time course of PDE*. In Fig. 3A, the amplitudes and durations of the PDE* pulses from three samples of unwashed ROS increase slightly as the free calcium level is raised from 10 to 500 and to 1000 nM. Kinetically, this effect is reminiscent of that shown in Fig. 1A, where ROS are enriched in RK. Namely, the rising and falling slopes of the three pulses being identical, the increase in peak amplitude appears to come from a delay in the onset of deactivation processes. In salamander (19) and gecko (20) rods, the rising slope of the photoresponse is steeper when the calcium increases. A careful analysis of these electrophysiological signals suggests that the catalytic activity of R* depends on calcium (19). The rising phase of our PDE* pulse, which is

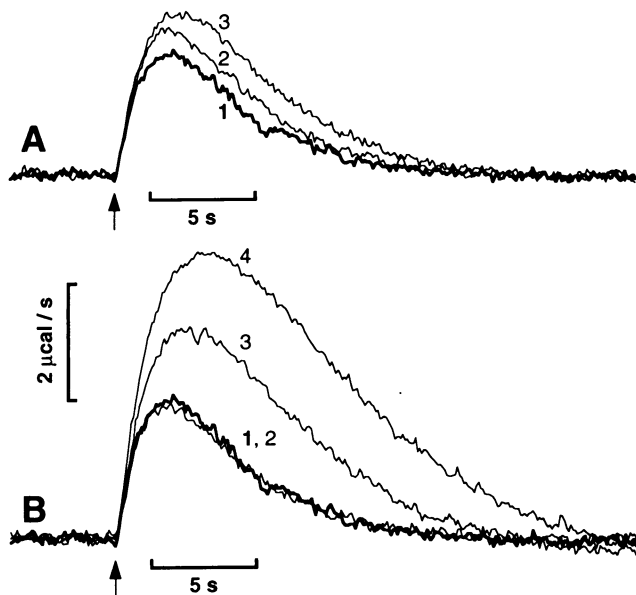
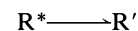
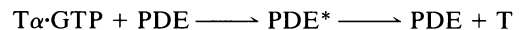
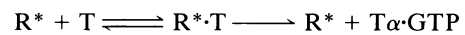


FIG. 3. The effect of calcium and recoverin. The ROS (100 μM rhodopsin) were unwashed. $[\text{R}^*] = 45 \text{ R}^*/\text{rod}$. All thick traces (labeled 1) are controls with 10 nM free Ca^{2+} and no proteins added. (A) No proteins were added to the two test aliquots and their free Ca^{2+} levels were 500 nM (trace 2) and 1 μM (trace 3). (B) Five μM myristoylated (14:0) recoverin were added to the three test aliquots whose free Ca^{2+} levels were 10 nM (trace 2), 500 nM (trace 3), and 1 μM trace (4).

closely related to the activation of transducin by R* (see below), is, however, totally insensitive to calcium. Lagnado and Baylor (19) think that this calcium regulation of R* activity relies on a soluble fraction, which could have been lost during the preparation of our ROS, thus accounting for our negative result.

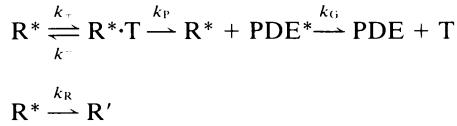
Recoverin is the most obvious protein that could mediate this calcium-provoked lengthening of the PDE* pulse. From the gel of Fig. 1, the endogenous level of recoverin in the samples of Fig. 3A is estimated at 1 μM . Many recent *in vitro* experiments indicate that at high Ca^{2+} , recoverin inhibits the phosphorylation of R* presumably by interacting with rhodopsin kinase (6, 14, 21–23). In Fig. 3B, unwashed ROS are complemented with 5 μM myristoylated (14:0) recoverin, which has absolutely no effects at 10 nM free calcium (traces 1 and 2). However, when the free calcium is raised to 500 nM (trace 3) [i.e. the level found in a dark-adapted outer segment (20)], the pulse of PDE* undergoes a significant 50% increase in peak amplitude and duration. The effect is, however, far from being saturated as it can be extended much further when the free Ca^{2+} level is boosted to 1 μM . For the incorporation of phosphate into R*, the calcium half-saturation point was first reported to be 140–250 nM (6, 22, 23), i.e. within the physiological range. However, more recent studies have shown that this half-saturation point is in the micromolar range (14, 21). For the binding of recoverin to stripped ROS, the half-saturation point is also 1–2 μM (24, 25), while for the binding of calcium to recoverin it is 17 μM (26). Amidst these very different results, our finding that there is an effect by exogenously added recoverin within the physiological range—even if its saturation lies without—stands together with the report by Gray-Keller *et al.* (5) that recoverin delays the recovery of the gecko rod's photoresponse. In their experiments, the calcium level was necessarily physiological as the rod cell was functionally intact. Moreover, their effect resembles ours, in both extent and nature; there is a 50–70% increase in duration and peak amplitude, while the rising and falling slopes are unchanged.

A Kinetic Model for the Competition Between RK and Transducin for R*. In Fig. 1, enrichment with rhodopsin kinase enhances R* deactivation while omitting ATP discourages it. In Fig. 3, this deactivation was delayed by the calcium-dependent action of exogenous recoverin. In all of these experiments, whenever R* quenching is made more efficient, the pulse of PDE* gets shorter and smaller but the rising slope is always preserved. The falling slope is also unchanged in most cases. This kinetic behavior suggests that when R* is shut off less efficiently, the onset of deactivation is delayed and the activation phase is allowed to go on longer, giving an increase in pulse duration and amplitude. At these low light levels, each R* is alone on a membrane fragment and its interaction with the surrounding ocean of transducin is favored, to the detriment of a rarer species such as RK. We formulate this unequal competition between RK and transducin as follows



with $\text{T} = \text{T}\beta\gamma\text{-T}\alpha\text{-GDP}$; $\text{PDE} = \text{holoPDE}$; $\text{PDE}^* = \text{T}\alpha\text{-GTP-holoPDE}$; and $\text{R}' = \text{phosphorylated and capped R}^*$. R* appears instantaneously with the light flash at some initial level R_0 ; it activates transducin in a classic Briggs-Haldane scheme. PDE is turned on by association with $\text{T}\alpha\text{-GTP}$ and is deactivated in one step upon GTP hydrolysis by $\text{T}\alpha$. For simplicity, the many-step deactivation of R* is condensed into one step where the actions of RK and arrestin/p44 are only implied. We assume that the association of PDE to $\text{T}\alpha\text{-GTP}$ is

faster than the latter's dissociation from $R^* \cdot T$. Without this assumption, the algebra is more complex but the same kinetic conclusions are reached. Finally, as the fraction of active PDE is less than 1% (see above), we treat T and PDE as constants. We now write



The constant transducin concentration T_0 is incorporated into k_+ : $k_+ = k_b \cdot T_0$, for some bimolecular rate constant k_b . PDE^* is now the product of the catalytic activation of transducin by R^* , with k_P as the turnover number. Henceforth, transducin activation will equivalently mean PDE activation. The rate constant k_G for the GTPase-dependent deactivation of PDE^* is about 1 s^{-1} (3).

The enzymatic activation of transducin by R^* is saturated because the transducin concentration on the disc is $\sim 10\%$ R , while the Michaelis constant K_M is only 2% R (27). Substrate saturation of an enzyme has two equivalent well known meanings. (i) At steady state, the product appears with a rate that is proportional to the amount of enzyme and to k_{cat} , the turnover number. (ii) The enzyme is practically never free but is most of the time bound up in the enzyme-substrate complex. With this latter feature in mind, we immediately see that in our case, the accessibility of kinase to R^* is drastically reduced on account of R^* being sequestered in the $R^* \cdot T$ complex most of the time. Consequently, the level of R^* remains close to its initial value R_0 for quite awhile after the light flash. During this delay, production of PDE^* proceeds at a rate that is proportional to the amount of enzyme R_0 and to k_P . It is this rate, which is independent of R^* deactivation, that determines the constant rising slope of our signals. The level of R^* has no influence on the slope of the rising phase but only on how soon this phase terminates once R^* has fallen significantly below R_0 . From this discussion, k_+ must be much larger than both k_P and k_R . Recall that $k_+ = k_b \cdot T_0$; $T_0 = 10\%$ R ; $K_M = 2\%$ R ; and $k_P \approx k_{cat} = 800 \text{ s}^{-1}$, which is the turnover number for transducin activation by R^* (27). By recognizing that $k_b > k_{cat}/K_M$, it is easy to see that $k_+ > 4000 \text{ s}^{-1}$ and therefore $k_+ > k_P$. As for the difference between k_+ and k_R , it is huge since k_R cannot be much more than a few s^{-1} .

Our simplified kinetic scheme can be solved to obtain $PDE^*(t)$ as a function of time:

$$PDE^*(t) = \frac{R_0 k_+ k_P}{\Delta} \left[\frac{e^{-\lambda_1 t}}{k_G - \lambda_1} - \frac{e^{-\lambda_2 t}}{k_G - \lambda_2} + \frac{\Delta e^{-k_G t}}{(k_G - \lambda_1)(k_G - \lambda_2)} \right]$$

$$\Delta = \sqrt{(k_+ + k_- + k_P + k_R)^2 - 4k_R(k_- + k_P)}$$

$$\approx k_+ + k_- + k_P + k_R \approx k_+$$

$$\lambda_1 = \frac{(k_+ + k_- + k_P + k_R) - \Delta}{2}$$

$$\approx \frac{(k_- + k_P)}{(k_+ + k_- + k_P + k_R)} k_R \approx 1 - 2 \text{ s}^{-1}$$

$$\lambda_2 = \frac{(k_+ + k_- + k_P + k_R) + \Delta}{2}$$

$$\approx (k_+ + k_- + k_P + k_R) \approx 5000 \text{ s}^{-1}$$

We implied above that during the rising phase, the production of PDE^* follows a steady-state regime. This is reached after a

characteristic time of $1/\lambda_2$, which is much less than 1 ms. The other two characteristic times, $1/\lambda_1$ and $1/k_G$, being on the order of 1 s, the $1/\lambda_2$ exponential in the expression for PDE^* quickly drops out and for most of the signal's duration we have:

$$PDE^*(t) \approx \frac{R_0 k_+ k_P}{\Delta(k_G - \lambda_1)} (e^{-\lambda_1 t} - e^{-k_G t}), \text{ for } t > \frac{1}{\lambda_2} \quad [2]$$

Since λ_1 and k_G are comparable, we can linearly expand the exponentials to extract the behavior of $PDE^*(t)$ during its rising phase:

$$PDE^*(t) \approx \frac{R_0 k_+ k_P}{\Delta} t \approx \frac{R_0 k_+ k_P}{(k_+ + k_- + k_P + k_R)} t$$

$$\approx R_0 k_P t, \text{ for } t < \frac{1}{\lambda_1}, \frac{1}{k_G} \quad [3]$$

This confirms that the rising slope is directly proportional to the illumination level R_0 , the proportionality constant being k_P , the rate constant for the production of PDE^* . Moreover, this rising phase is independent of k_R , i.e. of the deactivation of R^* . The time evolution of photoactivated rhodopsin is:

$$R(t) + R^* \cdot T(t) = \frac{R_0}{\Delta} \{ (k_+ + k_- + k_P - \lambda_1) e^{-\lambda_1 t} - (k_+ + k_- + k_P - \lambda_2) e^{-\lambda_2 t} \} \approx \frac{R_0}{\Delta} (k_+ - \lambda_1) e^{-\lambda_1 t} \quad [4]$$

The approximation, made possible because $\lambda_2 \gg \lambda_1$, clearly reveals that the R^* deactivation rate is not k_R but λ_1 , which is k_R modulated by a factor that depends on k_+ , i.e. on the abundance of transducin (see Eq. 1).

Equation 1 was fitted to the control trace of Fig. 1A. At each iteration, the computed curve was convolved with the impulse response of the instrument and compared with the experimental curve. The flat residual illustrates the excellent goodness of fit. Because k_+ , k_- , k_P , and k_R appear often in Eq. 1 as

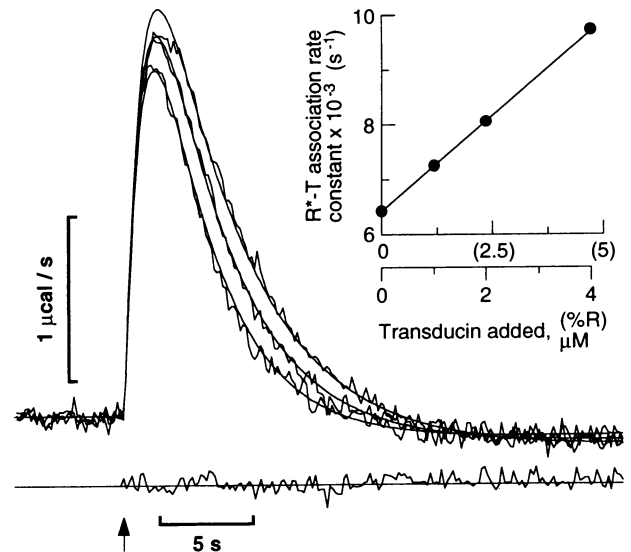


FIG. 4. Enrichment with exogenous transducin. $[free \text{ Ca}^{2+}] = 10 \text{ nM}$; $[R^*] = 45 \text{ R}^*/\text{rod}$. The three pulses of PDE^* (noisy traces) are from three aliquots containing, from bottom to top, 0, 2, 4 μM exogenous transducin. The fits (smooth traces) are computed as described in the text. The residual belongs to the fit of the PDE^* pulse with 2 μM transducin added. (Inset) The association rate constant (k_+ , see text) from the fitted traces are plotted as a function of added transducin. (The signal from the aliquot with 1 μM exogenous transducin is omitted for clarity.)

sums, very different sets of these parameters can give the same excellent fit. We thus require two extra conditions: $k_+ > 4000 \text{ s}^{-1}$ (see above) and k_+ , k_P , and k_- must approximately satisfy the definition of K_M , i.e., $k_+ \approx (k_P + k_-) T_0/K_M$. With these constraints, we obtain $k_+ = 7800 \text{ s}^{-1}$; $k_- = 690 \text{ s}^{-1}$; $k_P = 880 \text{ s}^{-1}$; $1/k_R = 0.6 \text{ s}$; and $1/k_G = 1 \text{ s}$, which is the time of PDE* deactivation and is comparable with the previously reported value of 0.73 s (3). As for k_+ , it is indeed much larger than k_R and is comparable with some theoretical values reported elsewhere (28, 29). The value of k_P is close to the turnover number of 800 s^{-1} for the activation of transducin by R^* (27). If the intrinsic R^* lifetime $1/k_R$ is only 0.6 s, the effective R^* lifetime $1/\lambda_1$ is 3 s. Equation 1 was next fitted to trace 4 (RK and arrestin added) by allowing k_R to vary while fixing k_+ , k_- , k_P , and k_G at their previous values. The value for $1/k_R$ is now 0.4 s, while the goodness of fit has worsened somewhat as judged from the residual. This small change in $1/k_R$ is compatible with the previous observation that the falling phases of traces 1 and 4 are pretty much the same.

We can predict from our model the effects of enriching the ROS with transducin; the activation phase being already saturated, the rising slope should be unaffected, but rhodopsin kinase should have even less access to R^* and the PDE* pulse should therefore widen. This is indeed the case as shown in Fig. 4. The rising slope is strictly preserved even though the transducin level has increased by as much as 50%, showing that activation by R^* is indeed substrate-saturated. But the pulse width steadily increases as more transducin is added; it has become harder and harder for RK to get to R^* . Fitting Eq. 1 to the trace with $2 \mu\text{M}$ exogenous transducin yields $k_+ = 8000 \text{ s}^{-1}$; $k_- = 770 \text{ s}^{-1}$; $k_P = 850 \text{ s}^{-1}$; $1/k_R = 0.9 \text{ s}$; and $1/k_G = 1 \text{ s}$. Then, the other traces can be fitted rather well by allowing only k_+ to vary. Moreover, the k_+ thus obtained increases linearly with the transducin added (Fig. 4 inset), which is as expected since $k_+ = k_b T_0$.

Recently, Chen *et al.* (30) obtained single photon responses from mouse rods where some of the rhodopsin molecules were unquenchable because they lacked part of the C terminus. A response elicited by photoactivation of a truncated R^* differs from a normal one in its duration and amplitude but not in its rising slope. This kinetic feature is reminiscent of what we saw when we omitted ATP, and Chen *et al.* (30) also concluded that R^* quenching prematurely terminates the activation phase. As said above, when Gray-Keller *et al.* (5) dialyzed recoverin into gecko rods, their effect is identical to ours when we add recoverin to the ROS suspension: an increase in duration and amplitude but no change in rising slope. Thus, our time-resolved biochemical measurements directly link these electrophysiological results to the underlying amplification cascade. Moreover, our kinetic model, by quantitatively describing the lopsided competition between transducin and RK, explains how the deactivation of R^* truncates the rising phase.

CONCLUSION

At 37°C , the photoresponse of a mammalian rod lasts $\sim 0.3 \text{ s}$ (FWHM) (30, 31). As measured here at 23°C , the light-induced PDE activity from a ROS suspension where the quenching of R^* is maximal, lasts 4 s. Hence, this difference in kinetics might be in part a temperature effect. (For technical reasons, we cannot yet do our measurements at 37°C .) The slowness of the photoresponse in amphibians is usually attributed to low body temperatures (29). It is also possible that in the rod, the guanylate cyclase is stimulated early enough so that the cGMP-gated channels reopen before the PDE is fully reinitiated. While *in vitro*, purified, or recombinant recoverin clearly affects the activity of RK, the role of endogenous recoverin *in vivo* remains ill defined, not least because the calcium

dependence of the *in vitro* studies is so puzzling. Here, we tend to use exogenous recoverin as an opportunistic tool to modulate the deactivation of R^* in our endeavor to understand its kinetic features. Whether our recoverin results have any bearing on the *in vivo* situation must await further experimentation.

What is the lifetime of R^* ? This innocent question implies an intrinsic deactivation of R^* by RK and the capping proteins that is free, isolated, and unhindered. Such a lifetime would be $1/k_R$ in our model. But the quenching of R^* is very much hindered, for RK must contend with the hugely abundant transducin for access to R^* . This interference by transducin gives rise to an effective lifetime $1/\lambda_1$ for R^* , which is five times longer than the intrinsic $1/k_R$. With this unfair competition, Nature has constructed an invariant rising phase for PDE* production separate and distinct from all deactivation processes.

We thank J. Bigay and A. Otto-Bruc for helping with some experiments, I. Lenoir for preparing rod outer segments, and Nordine Belmokhtar for building the microcalorimeter. This work was supported in part by National Institutes of Health Grant EY01730 to K.P.; by a grant from Research to Prevent Blindness to the Department of Ophthalmology to U.W.; and by a Human Frontier Science Program Organization grant to K.P., J.B.H., and T.M.V. K.P. is a recipient of a Jules and Doris Stein Research to Prevent Blindness Professorship.

1. Baylor, D. A., Lamb, T. D. & Yau, K.-W. (1979) *J. Physiol.* **288**, 613–634.
2. Lagnado, L. & Baylor, D. A. (1992) *Neuron* **8**, 995–1002.
3. Vuong, T. M. & Chabre, M. (1991) *Proc. Natl. Acad. Sci. USA* **88**, 9813–9817.
4. Wilden, U., Hall, S. W. & Kühn, H. (1986) *Proc. Natl. Acad. Sci. USA* **83**, 1174–1178.
5. Gray-Keller, M. P., Polans, A. S., Palczewski, K. & Detwiler, P. B. (1993) *Neuron* **10**, 523–531.
6. Kawamura, S. (1993) *Nature* **362**, 855–857.
7. Palczewski, K., Buczylo, J., Ohguro, H., Annan, R. S., Carr, S. A., Crabb, J. W., Kaplan, M. W., Johnson, R. S. & Walsh, K. A. (1994) *Protein Science* **3**, 314–324.
8. Smith, W. C., Milam, A. H., Dugger, D., Arendt, A., Hargrave, P. A. & Palczewski, K. (1994) *J. Biol. Chem.* **269**, 15407–15410.
9. Catty, P., Pfister, C., Bruckert, F. & Deterre, P. (1992) *J. Biol. Chem.* **267**, 17489–17493.
10. Liebman, P. A. & Evanczuk, T. (1982) *Methods Enzymol.* **81**, 532–542.
11. Kühn, H. (1981) *Curr. Top. Membr. Transp.* **15**, 171–201.
12. Tsien, R. & Pozzan, T. (1989) *Methods Enzymol.* **172**, 230–262.
13. Buczylo, J. & Palczewski, K. (1993) *Methods Neurosci.* **15**, 226–236.
14. Chen, C.-K., Inglese, J., Lefkowitz, R. J., and Hurley, J. B. (1995) *J. Biol. Chem.* **270**, 18060–18066.
15. Ray, S., Zozulya, S., Niemi, G. A., Flaherty, K. M., Brolley, D., Dizhoor, A. M., Mckay, D. B., Hurlley, J. B. & Stryer, L. (1992) *Proc. Natl. Acad. Sci. USA* **89**, 5705–5709.
16. Wensel, T. G. & Stryer, L. (1990) *Biochemistry* **29**, 2155–2161.
17. Hagins, W. A., Ross, P. D., Tate, R. L. & Yoshikami, S. (1989) *Proc. Natl. Acad. Sci. USA* **86**, 1224–1228.
18. Peitzsch, R. M. & McLaughlin, S. (1993) *Biochemistry* **32**, 10436–10443.
19. Lagnado, L. & Baylor, D. A. (1994) *Nature* **367**, 273–277.
20. Gray-Keller, M. P. & Detwiler, P. B. (1994) *Neuron* **13**, 849–861.
21. Klenchin, V. A., Calvert, P. D. & Bownds, M. D. (1995) *J. Biol. Chem.* **270**, 16147–16152.
22. Gorodovikova, E. N., Gimelbrandt, A. A., Senin, I. I. & Philippov, P. P. (1994) *FEBS Lett.* **349**, 187–190.
23. Gorodovikova, E. N., Senin, I. I. & Philippov, P. P. (1994) *FEBS Lett.* **353**, 171–172.
24. Zozulya, S. & Stryer, L. (1992) *Proc. Natl. Acad. Sci. USA* **89**, 11569–11573.
25. Dizhoor, A. M., Chen, C.-K., Olshevskaya, E., Sinelnikova, V. V., Philippov, P. & Hurley, J. B. (1993) *Science* **259**, 829–832.
26. Ames, J. B., Porumb, T., Tanaka, T., Ikura, M. & Stryer, L. (1995) *Biochemistry* **270**, 4526–4533.
27. Bruckert, F., Chabre, M. & Vuong, T. M. (1992) *Biophys. J.* **63**, 616–629.
28. Lamb, T. D. & Pugh, E. N., Jr. (1992) *J. Physiol.* **449**, 719–757.
29. Lamb, T. D. (1994) *Biophys. J.* **67**, 1439–1454.
30. Chen, J., Makino, C. L., Peachey, N. S., Baylor, D. A. & Simon, M. I. (1995) *Science* **267**, 374–377.
31. McNaughton, P. A. (1990) *Physiol. Rev.* **70**, 847–883.